Received: 3 February 2021 | Revised: 27 May 2021 | Accepted: 6 June 2021

DOI: 10.1111/jmg.12626

ORIGINAL ARTICLE

Journal of METAMORPHIC GEOLOGY WILEY

GeoPS: An interactive visual computing tool for thermodynamic modelling of phase equilibria

Hua Xiang[1] | **James A. D. Connolly**[2]

[1]Institute of Geology, Chinese Academy of Geological Sciences, Beijing, China

[2]Department of Earth Sciences, Swiss Federal Institute of Technology, Zurich, Switzerland

Correspondence
Hua Xiang, Institute of Geology, Chinese Academy of Geological Sciences, Beijing 100037, China.
Email: xianghua2710@gmail.com

Funding information
National Natural Science Foundation of China, Grant/Award Number: 41972067

Abstract

The availability of thermodynamic data for geologically relevant phases has made practical the calculation of stable phase relations throughout the mantle and crust of terrestrial planets. GeoPS (http://www.geops.org) is a program designed for this purpose in which both input and output are done through an intuitive graphical user interface. GeoPS provides a wide range of phase equilibrium calculations based on a novel Gibbs energy minimization algorithm. The algorithm provides for exceptionally robust and computationally efficient solution to the phase equilibrium problem by successive alternation between a linear programming step to identify stable phase compositions and a nonlinear programming step to refine the compositions estimated during the linear programming. Applications include calculation of various types of phase diagrams and path-dependent phase fractionation. By combining an easy-to-use graphical user interface with a robust and efficient solver, GeoPS makes phase equilibrium modelling accessible to researchers and students with minimal training and provides a powerful tool for understanding natural phase relations and for planning experimental work.

KEYWORDS

metamorphism, phase diagram, phase equilibrium, thermodynamic modelling, visual computing

1 | INTRODUCTION

Accurate thermodynamic modelling of natural rocks is a challenging petrological task. In the past few decades, significant progress in the development of thermodynamic datasets and activity models for phases of petrological interest has been made, increasing our ability to predict complex assemblages, composition and phase relations (e.g., Berman, 1988; Helgeson et al., 1978; Holland et al., 2018; Holland & Powell, 1998, 2011; Naumov, Ryzhenko, & Khodakovsky, 1974; Powell & Holland, 1988; Stixrude & Lithgow-Bertelloni, 2011; White, Powell, Holland, et al., 2014). At present, there are numerous computer programs for calculation of equilibrium phase diagrams and/or phase diagram sections, based on different strategies. Among them, three are used widely by petrologists: THERMOCALC (Powell & Holland, 1988; Powell, Holland, & Worley, 1998), Perple_X (Connolly, 2009; Connolly & Kerrick, 1987), Theriak/Domino (de Capitani & Brown, 1987; de Capitani & Petrakakis, 2010). Each program has advantages and limits that have been summarized elsewhere (Connolly, 2017; Lanari & Duesterhoeft, 2019). However, one of their common characteristics is that they are implemented as console-based applications that are not user-friendly, especially for novice users. In this contribution, we present a new computational strategy that is implemented through an intuitive graphical user interface (GUI) named GeoPS.

GeoPS is a visual computing platform for phase equilibrium modelling based on Gibbs energy minimization. The platform anticipates a wide range of phase equilibrium calculations and provides appropriate graphical facilities. GeoPS can be used to compute the physicochemical properties of the stable phases of a system along a given pressure–temperature–composition (*P–T-x*) path or over a two-dimensional coordinate frame defined by such variables. The paper outlines the algorithm and provides examples to document the main functions, reliability and advantages of GeoPS.

2 | STRATEGY OF GEOPS

There are two strategies for the calculation of petrological phase diagram sections: phase equilibrium calculators (e.g., THERMOCALC, Powell, Holland, & Worley, 1998) and Gibbs energy minimization (e.g., Perple_X, Connolly, 1990; THERIAK-DOMINO, de Capitani & Brown, 1987). THERMOCALC computes the compositions of the phases for a specified phase assemblage but relies on user expertise to establish stability of the assemblage (Connolly, 2017; Lanari & Duesterhoeft, 2019; Powell, Holland, & Worley, 1998). Gibbs energy minimizers identify and characterize the stable phase assemblage from a list of potentially stable phases for a specified pressure, temperature and bulk composition. This method is used in GeoPS. Two-dimensional phase diagrams, or more commonly phase diagram sections, are then computed by mapping the phase relations over the variable coordinate frame of interest.

2.1 | The Gibbs energy minimization

In GeoPS, the Gibbs energy of the system is expressed as the sum of the Gibbs energies of all Π possible phases in the system:

$$G^{sys} = \sum_{j=1}^{\Pi} \alpha^j g^j, \tag{1}$$

where g^j is the molar Gibbs energy of phase j and α^j is the molar amount of the phase. In general the number of possible phases is far greater, indeed it may be infinite, than p, the number of equilibrium phases; however, Equation 1 remains valid in an equilibrium system because the amounts of all non-equilibrium phases are by definition zero. Mass balance further requires the molar compositions of the constituent phases satisfy

$$N_i^{sys} = \sum_{j=1}^{\Pi} \alpha^j n_i^j \; i = 1...c, \tag{2}$$

where n_i^j is the quantity of component i in the phase j and c is the number of independent chemical components.

The Gibbs energy minimization problem is to determine the proportion and composition of each of the phases that minimize the G^{sys} at constant P–T-x^{sys}. Gibbs energy minimization is a linear programming problem if the system consists of only stoichiometric phases (i.e., Π is finite). However, if solution phases are involved the problem becomes non-linear. In this case, the problem may be solved by either iterative non-linear programming (de Capitani & Brown, 1987; de Capitani & Petrakakis, 2010) or by linear programming after a linearization in which continuous solutions are approximated by a finite set of phase states (White, Johnson, & Dantzig, 1958) referred to as pseudocompounds (Connolly & Kerrick, 1987).

The complication in non-linear Gibbs energy minimization strategies is that they may converge to local minima, whereas the limitation of Gibbs energy minimization by linearization is that it becomes inefficient with the large numbers of pseudocompounds necessary to represent accurately the composition of complex solutions (Connolly, 2005). This problem is mitigated, but not eliminated, by successive linear programming (White, Johnson, & Dantzig, 1958; Connolly, 2009) in which the resolution of the linearization is increased around the putative stable compositions, that is, refinement points, identified after each linear programming step.

In this paper, we propose a hybrid Gibbs energy minimization algorithm that combines the strengths of both the linear scheme and the non-linear scheme through a series of linear and non-linear programming steps (Figure 1). The algorithm begins by solving the linearized Gibbs energy minimization problem, as in Perple_X, to obtain an initial approximation of the solution (Figure 1b).

The stable compositions of each solution model represented by the linearized solution as well the compositions of any metastable solutions that are close to the initial most stable assemblage are then refined by non-linear programming, as in THERIAK, by minimizing the energy of these solutions relative to the initial solution (Figure 1). The initial approximation defines the *g-x* plane (Figure 1a). The equation of state g^j of each phase can be transformed as

$$g^{\prime j} = g^j - \sum_{i=1}^{c} n_i^j \mu_i, \tag{3}$$

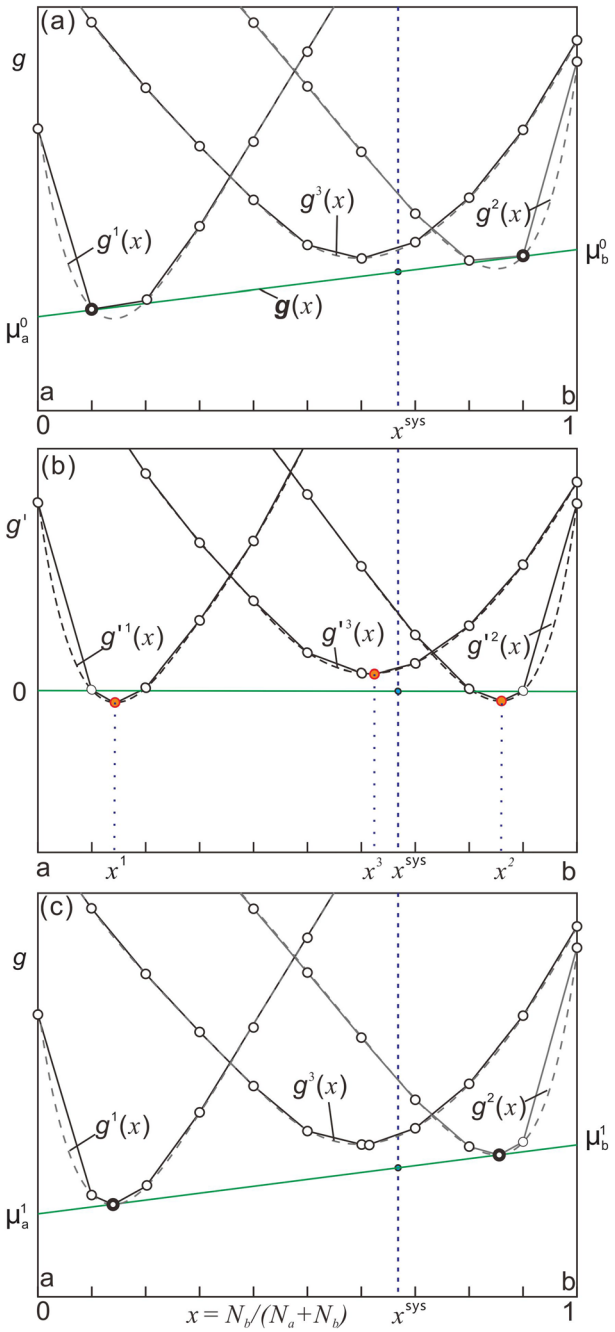

FIGURE 1 Schematic illustration of the GeoPS algorithm for a binary ($c = 2$), isobaric–isothermal, system with composition x^{sys}. (a) All possible states of matter are described by three solution phases $g^1(x)$, $g^2(x)$ and $g^3(x)$ (dashed curves). A finite set of points (circular symbols) are used to approximate the continuous equation of state of each solution phase. The initial solution (filled circles in a) is obtained by linear programming, and defines a g-x plane $g(x)$ and chemical potentials $\mu_a{}^0$ and $\mu_b{}^0$. (b) Given these chemical potentials, the g-coordinates of $g^1(x)$, $g^2(x)$ and $g^3(x)$ are transformed according to Equation (3). The minima in the transformed functions $g'^j(x)$ are then located by a simulated annealing method. And new points (filled circles) of these minima are added. (c) A new solution (filled circles in c) is obtained from these minima and the previous solution by linear programming. These steps are repeated iteratively until the phase compositions converge within the desired tolerance

where μ_i is the chemical potential of component i in the initial approximation and c is the number of independent chemical components. The minima of the individual g'^j functions are then located by a simulated annealing method (Bina, 1998; Kirkpatrick, Gelatt, & Vecchi, 1983); the coordinates of these minima untransformed and added to the list of pseudocompounds (Figure 1b); and the linear programming optimization is repeated (Figure 1c). This cycle of linear programming followed by non-linear optimization is repeated iteratively until the solution is judged to have converged to the global minimum.

2.2 | A strategy of adaptive refinement of triangular meshes for mapping phase diagram sections

In the mapping of phase diagram sections, a multilevel gridding strategy is needed to obtain high resolution in the vicinity of phase field boundaries without incurring high computational costs due to the needless use of high resolution within phase fields (e.g., Connolly, 2005). In GeoPS, an unstructured triangular grid that supports local adaptive mesh refinement is adopted (Figure 2). Firstly, the two-dimensional area to be calculated is divided into a M × N regular triangular lattice (Figure 2b). The equilibrium assemblage of each grid node is determined by Gibbs energy minimizer. If the same mineral assemblage is stable at three nodes of a triangle, then the mineral assemblage is assumed to be stable in the triangle. Likewise, heterogeneous triangles are marked for calculation in the next step. Each of these marked triangles is divided into two triangles, by adding a new node on the midpoint of the long side. At the same time, the neighbouring triangle also is divided into two triangles (Figure 2c). The stable mineral assemblage at each of the new nodes is predicted by the Gibbs energy minimizer, and heterogeneous triangles are again marked for subdivision and recalculation. These steps are repeated until the effective resolution, which is defined by the length of the long side of the triangle, reached the requirement (Figure 2d).

3 | DESCRIPTION OF THE PROGRAM

GeoPS is an interactive visual computing tool for phase equilibrium calculation (Figure 3) and can run on Windows OS with the.NET Framework 4.5 and later versions. The source code is written in MS Visual Basic. Net. The software and a tutorial are available online at

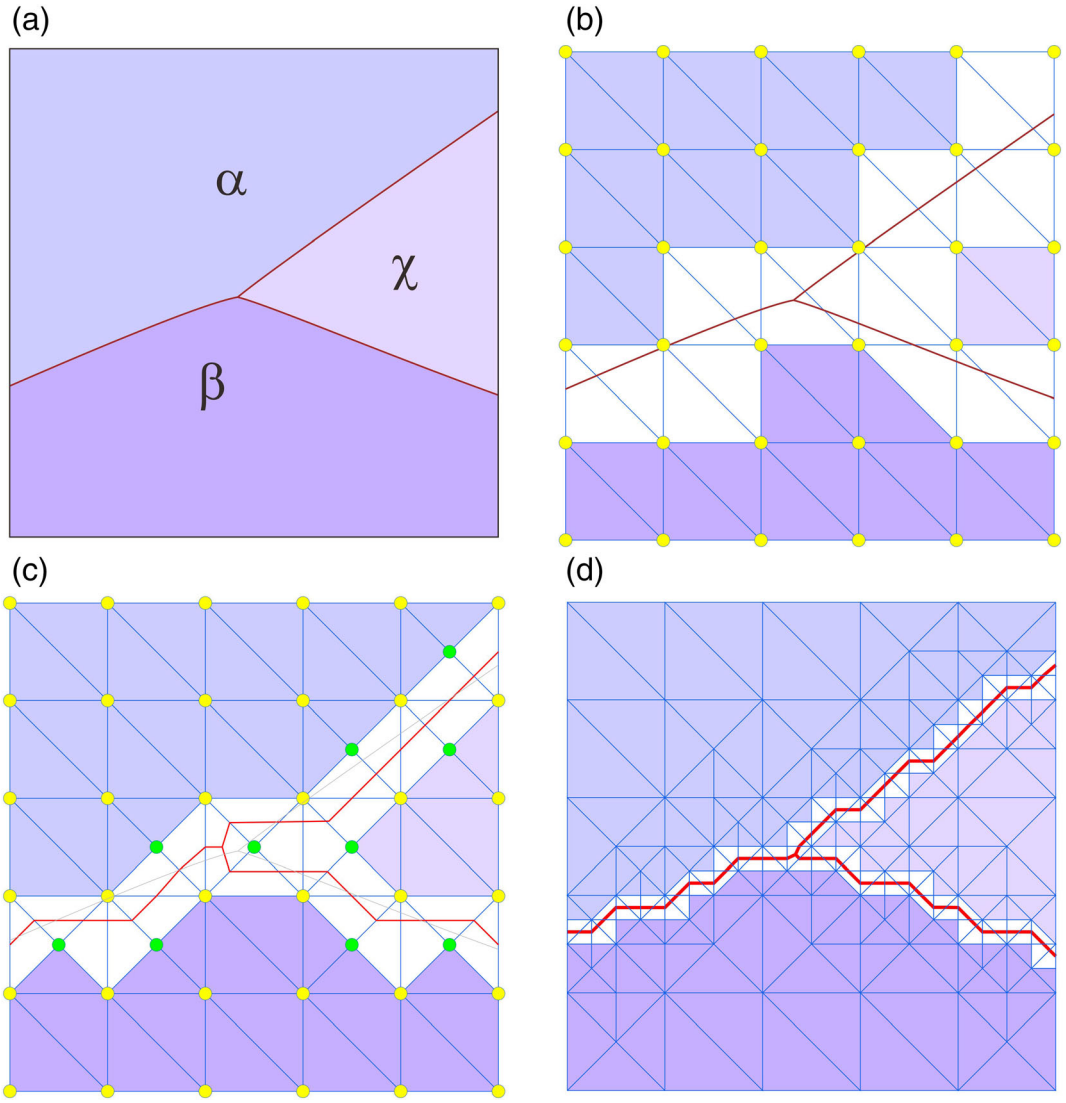

FIGURE 2 Sketch of the GeoPS algorithm. (a) Sample phase diagram. (b) Determining stable assemblages of each node in the initial grid and identifying which triangles need refinement. (c) Refining the marked triangles, determining stable assemblages of new nodes, and identifying which triangles need refinement. These steps are repeated iteratively until the effective resolution reached the requirement. (d) Shows the result after four steps are repeated

http://www.geops.org. GeoPS provides a series of functions for thermodynamic equilibrium calculations and illustration facilities. The type of computation and relevant physicochemical parameters, thermodynamic datasets and solution models are specified through a user-friendly interface (Figure 4).

Once the input has been completed, a preliminary graphical result is displayed immediately. This result is updated continuously until the requested effective resolution has been achieved (Figure 5). The resulting diagram can be exported in Scalable Vector Graphics (SVG) format or bitmap formats (e.g., JPG and BMP) as can be related to plots such as the mode and composition of phases. Alternatively, the underlying data can be exported in CSV format and analysed directly by the user.

3.1 | Relation between GeoPS and Perple_X

GeoPS and Perple_X have similar Gibbs energy minimization strategies; the innovation introduced in GeoPS is the use of non-linear programming to refine the estimated compositions of the stable phases during successive linear programming as in THERIAK (de Capitani & Brown, 1987). Prior to this innovation, Perple_X used a brute-force linear refinement strategy

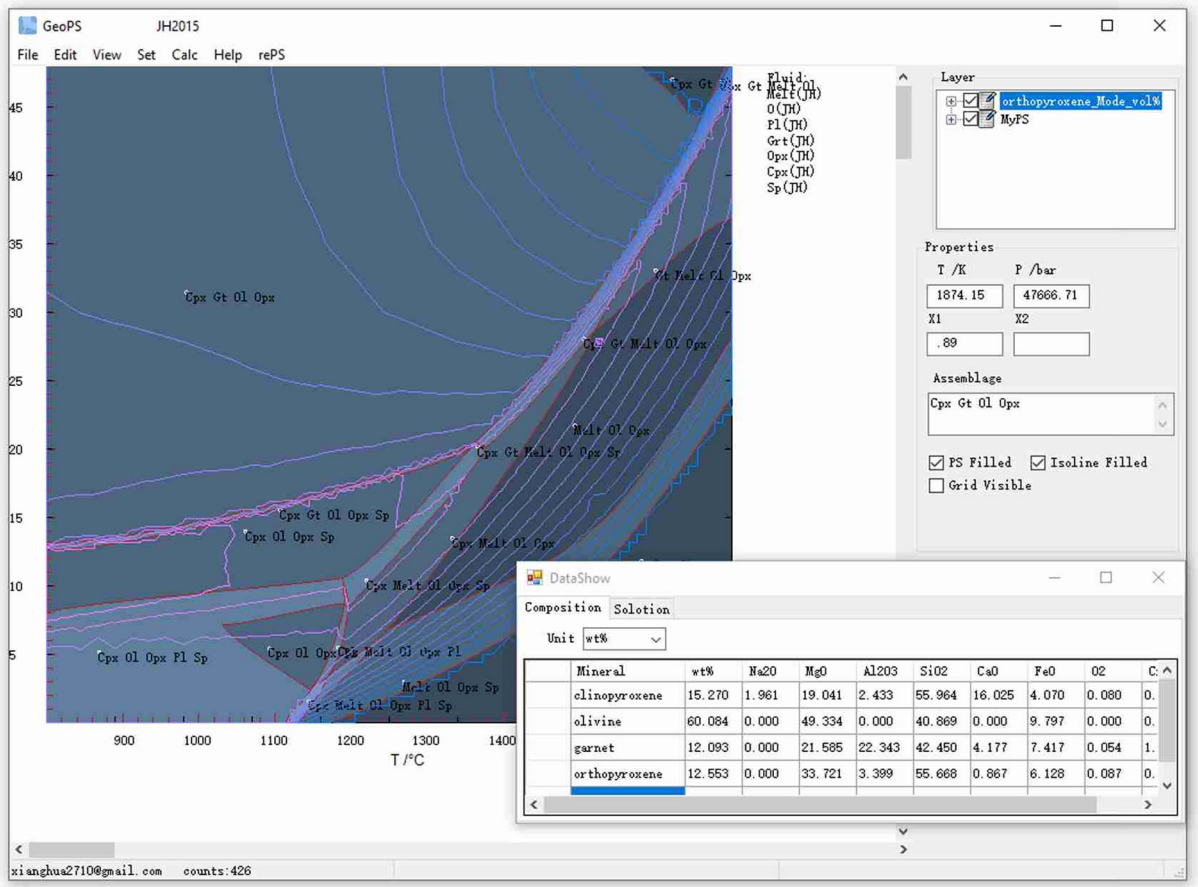

FIGURE 3 Screen image of the main interface of GeoPS. The displayed image is a *P–T* phase diagram section and isopleths of modal of Opx calculated for KLB-1 in the NCFMASOCr system, which bulk compositions are the same as Figure 1 of Jennings and Holland (2015). In the lower right is the 'DataShow' window which is interactively activated by selecting a point in the section and displays the relevant compositional data

(Connolly, 2009), which is computationally expensive for solution models with a large number of compositional variables. In the 6.9.1 revision of Perple_X, this linear strategy was replaced by a sequential quadratic programming algorithm (Gill, Murray, & Wright, 1981) that functionally corresponds to the use of the simulated annealing method (Bina, 1998; Kirkpatrick, Gelatt, & Vecchi, 1983) for the non-linear programming step of GeoPS. Thus, although the programs differ in detail, they offer comparable computational efficiency and precision. Because our goal here is to highlight GeoPS, in the comparisons made here we use the less efficient 6.9.0 version of Perple_X, benchmark comparisons with the 6.9.1 version are available online (http://www.perplex.ethz.ch). From a user perspective, the GUI of GeoPS is its greatest asset when compared with Perple_X. The GUI not only provides an intuitive guide for inexperienced users but also allows the interactive correction of poorly resolved portions of a calculated phase diagram section. The current capabilities of GeoPS are a subset of those available in Perple_X. Aside from this distinction, Perple_X offers a greater variety of thermodynamic models, and its code and data files are open-source.

4 | TESTS AND EVALUATION

4.1 | Benchmark calculations

To demonstrate the functionality and reliability of GeoPS, several published phase diagram sections created with THERMOCALC were reproduced with GeoPS and are discussed below.

4.1.1 | Phase diagram sections and isopleths

Metabasalt melting in the Na_2O—CaO—K_2O—FeO—MgO—Al_2O_3—SiO_2—H_2O—TiO_2—O_2 system (Figure 6a), this example reproduces the BL478 isochemical

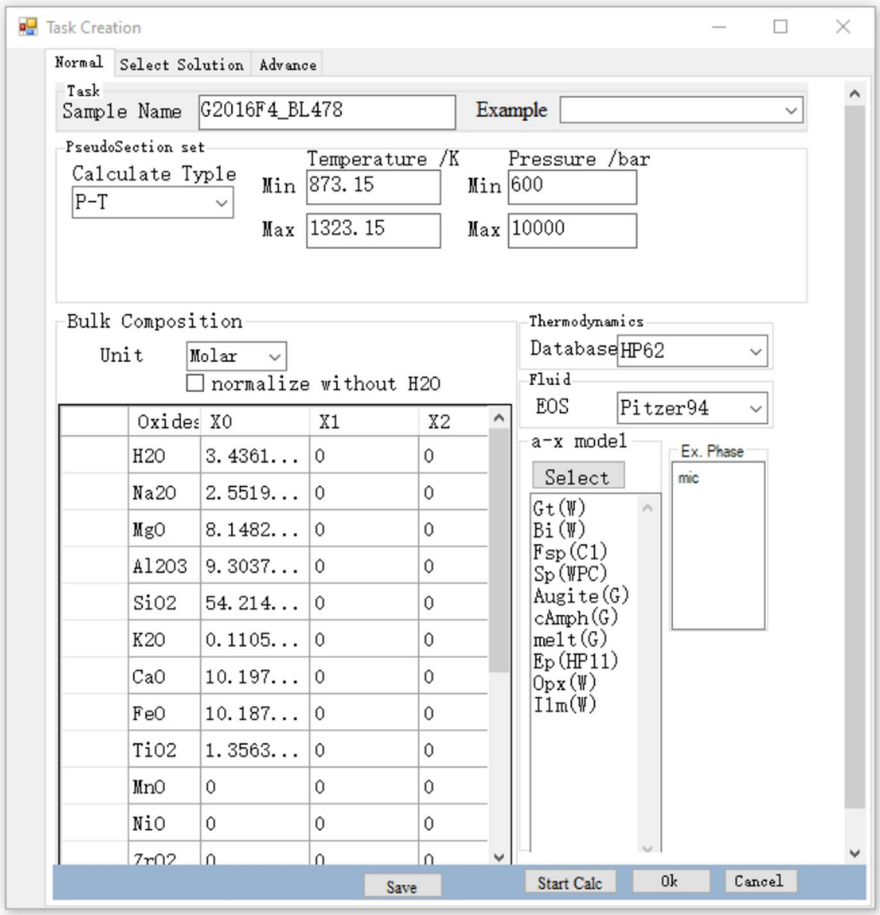

FIGURE 4 Screen image of a task creation interface

pressure–temperature section of Green et al. (2016), which was intended as a model for the phase relations of an experimental study by Beard and Lofgren (1991). The thermodynamic database and the activity models are those used in Green et al. (2016). The result shows that GeoPS quantitatively reproduces the phase relations in the BL478 section of Green et al. (2016) except in the low P–T corner of the section (Figure 6a),. In this region, the result from GeoPS is consistent with the results from Theriak-Domino and Perple_X (Supporting Information). Most likely the discrepancies with the section of Green et al. (2016) arise because biotite was not considered as a possible phase and the low-temperature orthopyroxene field was overlooked in the original calculation.

Suprasolidus metapelite melting in the MnO—Na_2O—CaO—K_2O—FeO—MgO—Al_2O_3—SiO_2—H_2O—TiO_2—O_2 system (Figure 6b): this example reproduces the suprasolidus phase relations of average amphibolite facies metapelite composition as calculated by White, Powell, and Johnson (2014). The thermodynamic database and the activity models are those of White, Powell, and Johnson (2014). The results of GeoPS are essentially identical to those obtained by White, Powell, and Johnson (2014) with THERMOCALC.

GeoPS can calculate *T*–*X* or *P*–*X* diagrams to investigate the effect of variable bulk chemistry. For example, an isobaric T–M_{H2O} (M_{H2O} is mol % of H_2O) section (Figure 7) shows the predicted effects of varying the H_2O content of the anhydrous equivalent of the BL478 composition mentioned previously (Figure 6a). This calculation reproduces the T–M_{H2O} section for BL478 in Green et al. (2016), as calculated by THERMOCALC, except at low T and M_{H2O}. Isopleths of the amount and/or compositions of phases are easily generated by GeoPS, for example, the isopleths of the anorthite content (X_{an}) of plagioclase as shown in Figure 7b.

4.1.2 | Path-dependent phase equilibrium modelling

GeoPS also can be used to calculate phase equilibrium along a given P–T path to investigate the variations of mineral properties during the metamorphism. Effective bulk composition (EBC) of the system can be altered

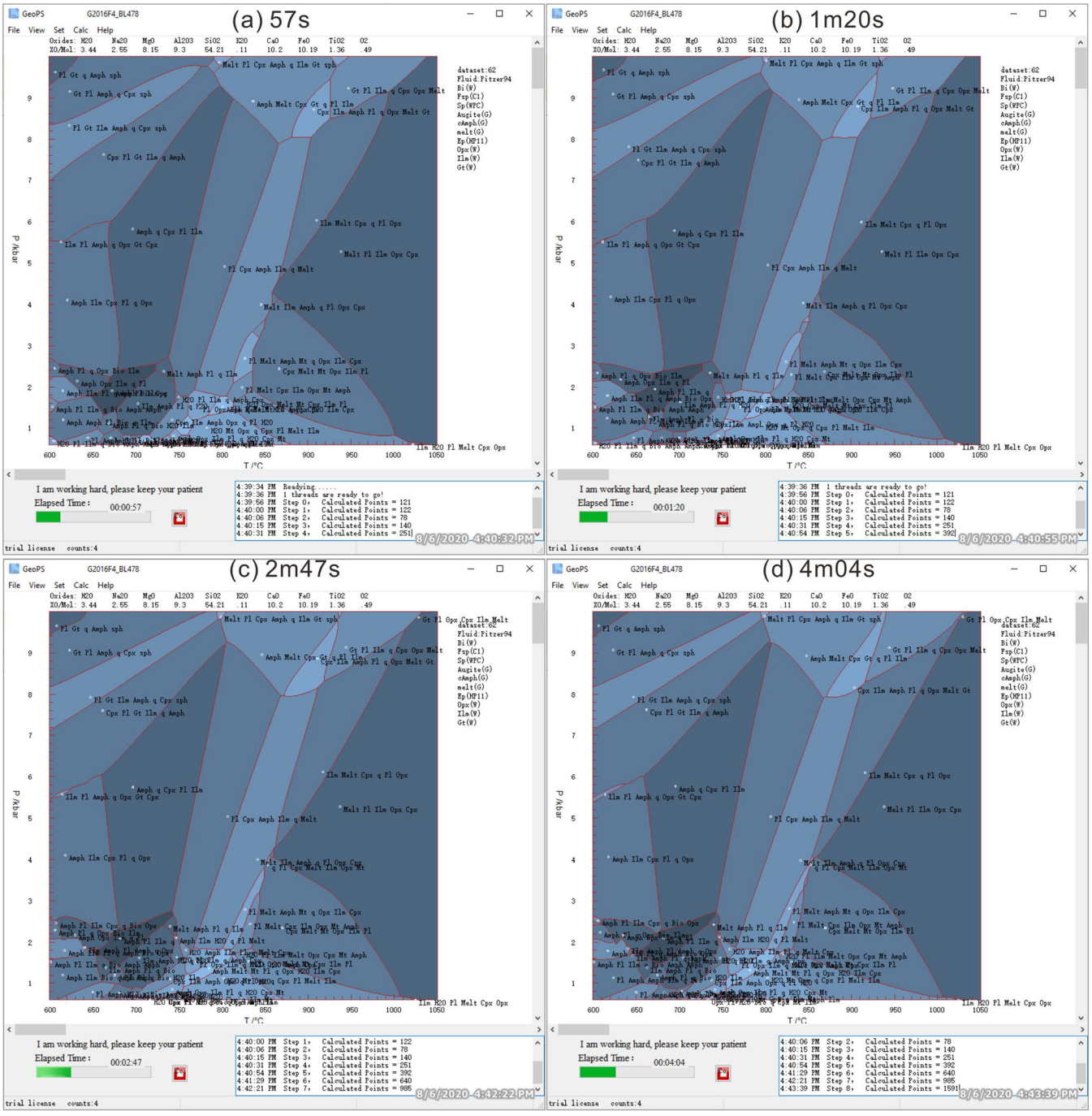

FIGURE 5 Screen images of the time evolution of a *P–T* phase diagram section (the BL487 section corresponding to Fig. 4a of Green et al., 2016) after for 57 s (a), 1 min and 20 s (b), 2 min and 47 s (c), and 4 min and 4 s (d). The example was calculated on a desktop with a 3.40-GHz Inter® Core™ i7-2600 CPU and 16 GB of RAM, Microsoft Windows 10 Pro ×64 operating system

throughout the metamorphic process, such as metamorphic dehydration and the volatile components escaping from the rocks on prograde segments, melt loss during the anatectic process (e.g. Mayne, Moyen, Stevens, & Kaislaniemi, 2016; Spear & Wolfe, 2018; White, Powell, & Holland, 2001; Yakymchuk & Brown, 2014). To show this functionality of GeoPS, a hypothetical clockwise P–T path (Figure 8a) is investigated with the BL478 starting bulk composition. Here, we calculated phase equilibrium along the P–T path with equilibrium model and melt loss/fractionation model, respectively. For the equilibrium model (Figure 8b), complete equilibrium at each step is assumed, the EBC of the system is invariant. For the fractionation model (Figure 8c), the EBC of the

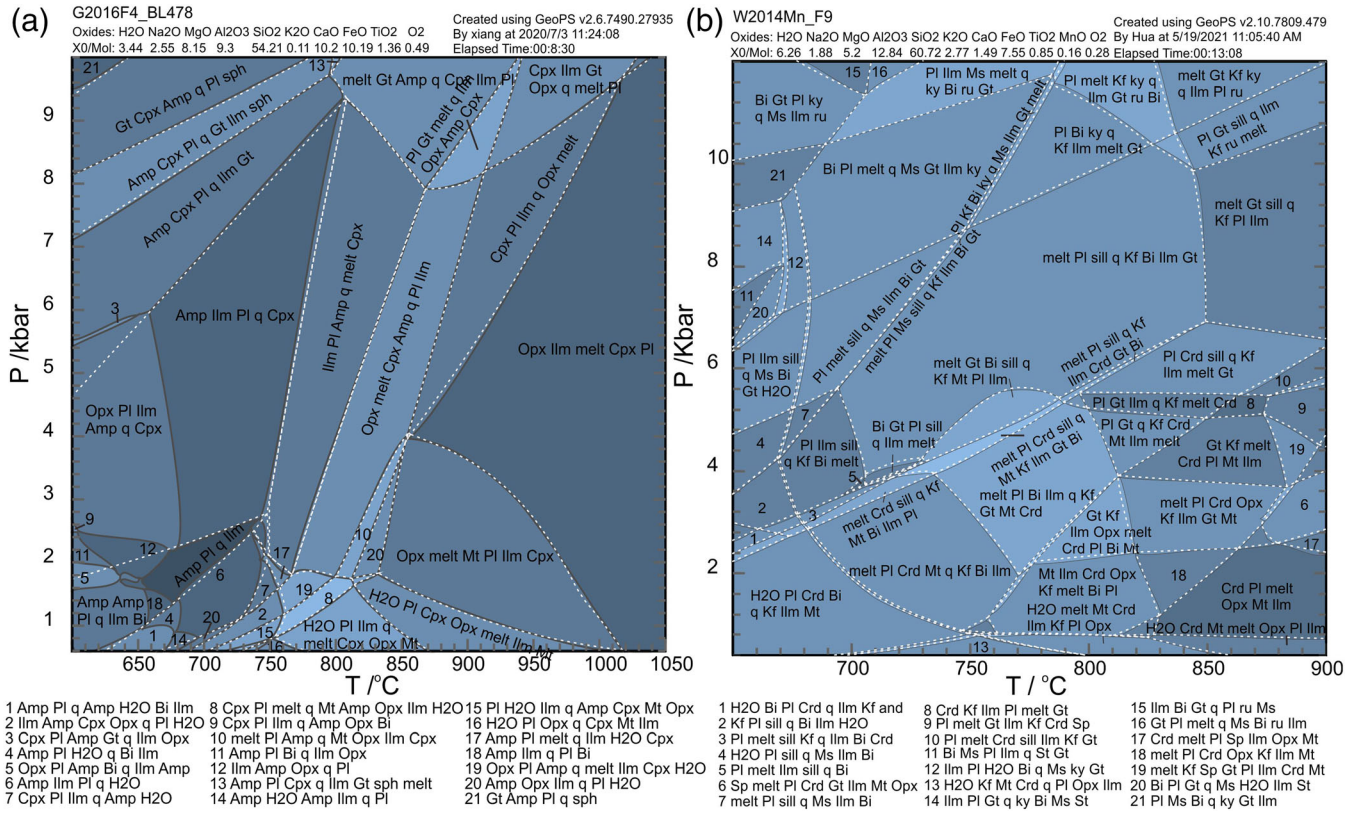

FIGURE 6 Comparisons of *P–T* phase diagram sections were calculated with THERMOCALC and GeoPS. (a) A *P–T* phase diagram section of a mafic sample created by GeoPS, the bulk composition is from Green et al. (2016). The dotted lines are from Fig. 4a of Green et al. (2016), which was calculated with THERMOCALC; (b) a *P–T* phase diagram section of pelitic rock created by GeoPS, the bulk composition is the same as used for Fig. 9 of White et al. (2014). The dotted lines are from Fig. 9 of White et al. (2014), which was calculated with THERMOCALC

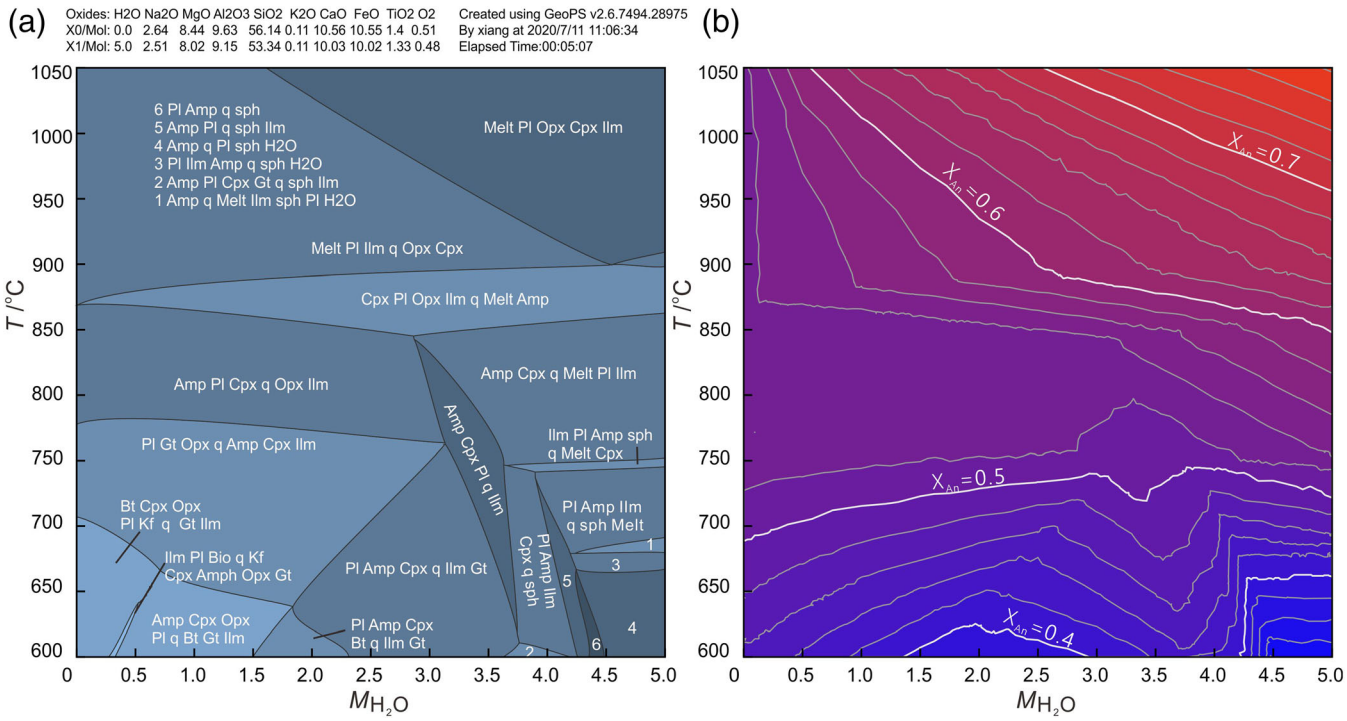

FIGURE 7 GeoPS calculated T–M_{H2O} section of sample BL478 at 7 kbar (a) and an isopleth of X_{an} of plagioclase (b)

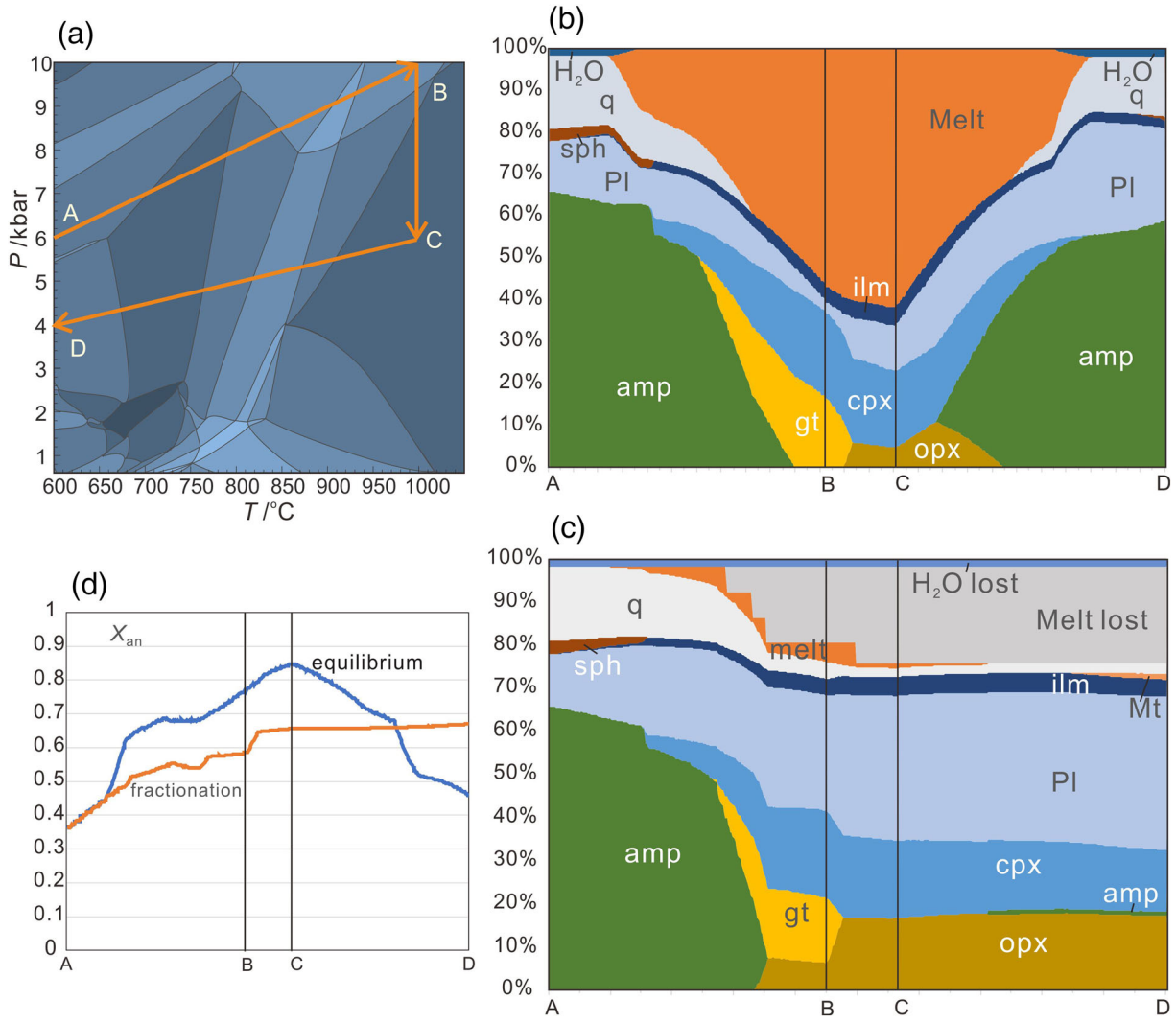

FIGURE 8 Phase equilibrium modelling for BL487 along a hypothetical clockwise *P*–*T* path. (a) the hypothetical clockwise *P*–*T* path; (b and c) phase proportions along the clockwise *P*–*T* path with equilibrium model (b) and fractionation model (c); (d) X_{an} of plagioclase along the clockwise *P*–*T* path

relative systems will change along the dependent path. Melt loss was set to occur when a 7-vol.% threshold of melt was exceeded and extraction left 1-vol.% melt. It is assumed that the free H_2O from metamorphic dehydration will escape from the system immediately.

Compared with the equilibrium model, the fractionation model has a significantly lower proportion of the cumulative total melt, a higher proportion of plagioclase and orthopyroxene at Points B and C. In the fractionation model, because melt loss cumulatively depletes residuum H_2O, the granulite facies mineral assemblage of Opx + Cpx + Pl are retained during retrograde cooling (Figure 8c), but with a small proportion of retrograde amphibole. Besides the differences in mineral assemblage and content between the fractionation model and the equilibrium model, there are also differences in mineral composition (Figure 8d).

4.2 | Computing efficiency

To quantify the computing speed of GeoPS, two computers were used as test platforms (Table 1). Computer-I is a laptop with a 2.60-GHz Inter® Core™ i7-6700HQ CPU and 16 GB of RAM, Microsoft Windows 10 Home ×64 operating system. Computer II is a desktop with a 3.40-GHz Inter® Core™ i7-2600 CPU and 16 GB of RAM, Microsoft Windows 10 Pro ×64 operating system. Several published *P*–*T* phase diagram sections for metapelitic, mafic and ultramafic rock compositions are used for benchmark testing. These benchmarks are also computed

TABLE 1 Computing time for several phase diagram sections using different computer programs

Fig.	*a-x* models	GeoPS computer I	GeoPS computer II	Perple_X v6.9.0[a]	Domino[b]
W14MnF9	Same with the Fig. 9 of White et al. (2014)	11 m 52 s; PR: <1 m	7 m 17 s; PR: ~50s	26 m 53 s	1 h 12 m 19 s
BL487a	Same with the Fig. 6a of Green et al., 2016	8 m 30 s; PR: ~1 m	6 m 31 s; PR: <1 m	14 h 35 m[c]	2 h 00 m 25 s
BL487b	Amph (DHP), no melt, Others are Green et al., 2016	1 m 49 s; PR: 30 s	1 m 10 s; PR: 20 s	9 m 29 s	
BL487c	Without solutions	22 s; PR: 3 s	19 s; PR: 2 s	2 s	
KLB-1	Jennings and Holland (2015)	8 m 01 s; PR: <1 m	3 m 41 s; PR: ~30s	20 m 18 s	

Abbreviation: PR, preliminary result.

[a]Using computer II. The initial_resolution value is [1/8 1/16]. All other option values are at default.

[b]Using Computer II. The executables of Theriak-Domino are from http://dtinkham.net/peq.html.

[c]The initial_resolution value is [1/6 1/12]. All other option values are at default.

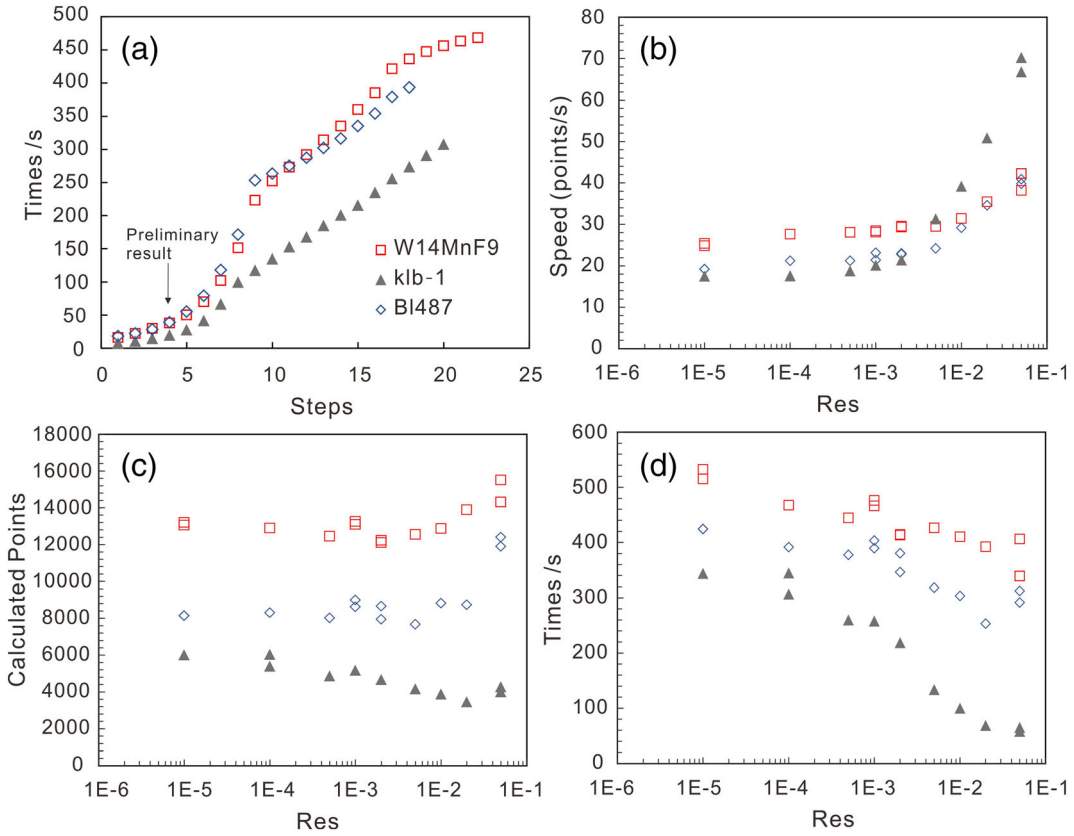

FIGURE 9 (a) A diagram of calculated time versus steps of grid refinement; (b) a diagram of calculated speeds (the number of calculated points per second) versus the compositional resolution of solutions. (c) Calculated points of each phase diagram sections at different compositional resolutions of solutions. (d) Calculated times of each phase diagram sections at different compositional resolutions of solutions

with Perple_X 6.9.0 and Theriak-Domino to demonstrate the computational speed of GeoPS.

Compared with Perple_X 6.9.0 and Theriak-Domino, for complex systems, GeoPS is orders of magnitude faster and of comparable, or better, quality (Table 1, Supporting Information). For simpler thermodynamic systems, GeoPS may be slower than Perple_X 6.9.0, but for such systems, the total time is short with either program and therefore the difference is of little consequence.

For GeoPS, the computing time and quality of results are controlled strongly by the grid resolution. Typically, GeoPS can give a preliminary result in a minute. If the grid resolution is higher, more refine steps and computing times are required (Figure 9a). Besides that, the compositional resolution of solutions will also affect computing speed and quality of results. The compositional resolution of solutions influences the precision of refining the compositions of the potential stable phases by iteration. With the decrease of solution resolution, the computing speed (the number of calculated equilibria per second) will decrease (Figure 9b). In general, the computing time will decrease with increasing solution resolution, although low resolution will lead to lower quality level of results and larger number of points requiring calculation (Figure 9c,d).

5 | CONCLUSIONS

GeoPS is a stand-alone GUI software that provides a wide range of phase equilibrium calculations based on a novel Gibbs energy minimization algorithm. The algorithm provides for robust and computationally efficient solution to the phase equilibrium problem. Applications include calculation of various types of phase diagrams and path-dependent phase fractionation. It can accomplish a phase diagram section in a few minutes even if the computation involves complex solution models; the speed is up to orders of magnitude faster than Perple_X and Theriak-Domino. For calculations from the same thermodynamic dataset and models, results from GeoPS are consistent with those obtained with other popular software, for example, THERMOCALC. By combining an intuitive GUI with a robust and efficient solver, GeoPS makes phase equilibrium modelling accessible to users with any level of expertise.

ACKNOWLEDGEMENTS

This paper was funded in part by the National Natural Science Foundation of China (41972067). Zeming Zhang, Zuolin Tian and Zhenyu He are thanked for their constructive suggestions about the GeoPS software. The development of the GeoPS software also was both actively and passively assisted by early users. We thank E. Green and an anonymous reviewer for their helpful reviews. We are also grateful R. White for the efficient editorial handling.

ORCID

Hua Xiang https://orcid.org/0000-0001-9221-7132

REFERENCES

Beard, J. S., & Lofgren, G. E. (1991). Dehydration Melting and Water-Saturated Melting of Basaltic and Andesitic Greenstones and Amphibolites at 1, 3, and 6. 9 kb. *Journal of Petrology*, *32*(2), 365–401. https://doi.org/10.1093/petrology/32.2.365

Berman, R. G. (1988). Internally-consistent thermodynamic data for minerals in the system Na_2O-K_2O-CaO-MgO-FeO-Fe_2O_3-Al_2O_3-SiO_2-TiO_2-H_2O-CO_2. *Journal of Petrology*, *29*, 445–522. https://doi.org/10.1093/petrology/29.2.445

Bina, C. R. (1998). Free energy minimization by simulated annealing with applications to lithospheric slabs and mantle plumes. In *Geodynamics of Lithosphere & Earth's Mantle* (pp. 605–618). Springer.

Connolly, J., & Kerrick, D. (1987). An algorithm and computer program for calculating composition phase diagrams. *Calphad*, *11*, 1–55. https://doi.org/10.1016/0364-5916(87)90018-6

Connolly, J. A. D. (1990). Multivariable phase diagrams; an algorithm based on generalized thermodynamics. *American Journal of Science*, *290*, 666–718. https://doi.org/10.2475/ajs.290.6.666

Connolly, J. A. D. (2005). Computation of phase equilibria by linear programming: A tool for geodynamic modeling and its application to subduction zone decarbonation. *Earth and Planetary Science Letters*, *236*, 524–541. https://doi.org/10.1016/j.epsl.2005.04.033

Connolly, J. A. D. (2009). The geodynamic equation of state: What and how. *Geochemistry, Geophysics, Geosystems*, *10*(Q10014), 1–19. https://doi.org/10.1029/2009gc002540

Connolly, J. A. D. (2017). A primer in Gibbs energy minimization for geophysicists. *Petrology*, *25*, 526–534. https://doi.org/10.1134/S0869591117050034

de Capitani, C., & Brown, T. H. (1987). The computation of chemical equilibrium in complex systems containing non-ideal solutions. *Geochimica et Cosmochimica Acta*, *51*, 2639–2652. https://doi.org/10.1016/0016-7037(87)90145-1

de Capitani, C., & Petrakakis, K. (2010). The computation of equilibrium assemblage diagrams with Theriak/Domino software. *American Mineralogist*, *95*, 1006–1016. https://doi.org/10.2138/am.2010.3354

Gill, P. E., Murray, W., & Wright, M. H. (1981). *Practical Optimization*. London: Academic Press. 401pp

Green, E., White, R., Diener, J., Powell, R., Holland, T., & Palin, R. (2016). Activity–composition relations for the calculation of partial melting equilibria in metabasic rocks. *Journal of Metamorphic Geology*, *34*, 845–869. https://doi.org/10.1111/jmg.12211

Helgeson, H. C., Delany, J. M., Nesbitt, H. W., & Bird, D. K. (1978). Summary and critique of the thermodynamic properties of rock-forming minerals. *American Journal of Science*, *278A*, 1–229.

Holland, T. J. B., & Powell, R. (1998). An internally consistent thermodynamic data set for phases of petrological interest. *Journal of Metamorphic Geology*, *16*(3), 309–343. https://doi.org/10.1111/j.1525-1314.1998.00140.x

Holland, T., & Powell, R. (2011). An improved and extended internally consistent thermodynamic dataset for phases of petrological interest, involving a new equation of state for solids. *Journal of Metamorphic Geology*, *29*, 333–383. https://doi.org/10.1111/j.1525-1314.2010.00923.x

Holland, T. J. B., Green, E. C. R., & Powell, R. (2018). Melting of peridotites through to granites: A simple thermodynamic model in the system KNCFMASHTOCr. *Journal of Petrology*, *59*, 881–900. https://doi.org/10.1093/petrology/egy048

Jennings, E. S., & Holland, T. J. (2015). A simple thermodynamic model for melting of peridotite in the system NCFMASOCr. *Journal of Petrology*, egv020, *56*, 869–892. https://doi.org/10.1093/petrology/egv020

Kirkpatrick, S., Gelatt, C. D., & Vecchi, M. P. (1983). Optimization by simulated annealing. *Science*, *220*(4598), 671–680. https://doi.org/10.1126/science.220.4598.671

Lanari, P., & Duesterhoeft, E. (2019). Modeling metamorphic rocks using equilibrium thermodynamics and internally consistent databases: Past achievements, problems and perspectives. *Journal of Petrology*, *60*, 19–56. https://doi.org/10.1093/petrology/egy105

Mayne, M., Moyen, J. F., Stevens, G., & Kaislaniemi, L. (2016). Rcrust: A tool for calculating path-dependent open system processes and application to melt loss. *Journal of Metamorphic Geology*, *34*, 663–682. https://doi.org/10.1111/jmg.12199

Naumov G. B., Ryzhenko B. N., & Khodakovsky I. L. (1974). Handbook of Thermodynamic Data. U.S. Department of Commerce, NTIS Report PB-226 722.

Powell, R., & Holland, T. (1988). An internally consistent dataset with uncertainties and correlations: 3. Applications to geobarometry, worked examples and a computer program. *Journal of Metamorphic Geology*, *6*, 173–204. https://doi.org/10.1111/j.1525-1314.1988.tb00415.x

Powell, R., Holland, T., & Worley, B. (1998). Calculating phase diagrams involving solid solutions via non-linear equations, with examples using THERMOCALC. *Journal of Metamorphic Geology*, *16*, 577–588. https://doi.org/10.1111/j.1525-1314.1998.00157.x

Spear, F. S., & Wolfe, O. M. (2018). Evaluation of the effective bulk composition (EBC) during growth of garnet. *Chemical Geology*, *491*, 39–47. https://doi.org/10.1016/j.chemgeo.2018.05.019

Stixrude, L., & Lithgow-Bertelloni, C. (2011). Thermodynamics of mantle minerals-II. Phase equilibria. *Geophysical Journal International*, *184*, 1180–1213. https://doi.org/10.1111/j.1365-246X.2010.04890.x

White, R., Powell, R., & Holland, T. (2001). Calculation of partial melting equilibria in the system Na_2O–CaO–K_2O–FeO–MgO–Al_2O_3–SiO_2–H_2O (NCKFMASH). *Journal of Metamorphic Geology*, *19*(2), 139–153. https://doi.org/10.1046/j.0263-4929.2000.00303.x

White, R., Powell, R., Holland, T., Johnson, T., & Green, E. (2014). New mineral activity–composition relations for thermodynamic calculations in metapelitic systems. *Journal of Metamorphic Geology*, *32*, 261–286. https://doi.org/10.1111/jmg.12071

White, R., Powell, R., & Johnson, T. (2014). The effect of Mn on mineral stability in metapelites revisited: New a–x relations for manganese-bearing minerals. *Journal of Metamorphic Geology*, *32*(8), 809–828. https://doi.org/10.1111/jmg.12095

White, W. B., Johnson, S. M., & Dantzig, G. B. (1958). Chemical equilibrium in complex mixtures. *The Journal of Chemical Physics*, *28*(5), 751–755. https://doi.org/10.1063/1.1744264

Yakymchuk, C., & Brown, M. (2014). Consequences of open-system melting in tectonics. *Journal of the Geological Society*, *171*(1), 21–40. https://doi.org/10.1144/jgs2013-039

SUPPORTING INFORMATION

Additional supporting information may be found online in the Supporting Information section at the end of this article.

Figure S1. A *P–T* phase diagram for BL487 calculated using GeoPS. The thermodynamic dataset used was Holland and Powell (2011), ds6.2. The a-x models are those used in Green et al. (2016). The dotted lines are from Fig. 4a of Green et al. (2016) which are calculated by THERMOCALC.

Figure S2. A *P–T* phase diagram for BL487 calculated using Perple_X. The thermodynamic dataset used was Holland and Powell (2011), ds6.2. The a-x models are those used in Green et al. (2016). The version of Perple_X is v6.9.0, the initial_resolution = [1/6, 1/12], all other option values are default. The dotted lines are from Fig. 4a of Green et al. (2016) which are calculated by THERMOCALC.

Figure S3. A *P–T* phase diagram for Bl487 calculated using Theriak-Domino. The thermodynamic dataset used was Holland and Powell (2011), ds6.2. The a-x models are those used in Green et al. (2016). The executables of Theriak-Domino are from http://dtinkham.net/peq.html. The dotted lines are from Fig. 4a of Green et al. (2016) which are calculated by THERMOCALC.

Figure S4. A *P–T* phase diagram for a metapelitic rock using GeoPS. The bulk composition is same as Fig. 9 of White et al. (2014b). The thermodynamic dataset used was Holland and Powell (2011), ds6.2. The a-x models are those used in White et al. (2014b),. The dotted lines are from Fig. 9 of White et al. (2014b) which are calculated by THERMOCALC.

Figure S5. A *P–T* phase diagram for a metapelitic rock using Perple_X. The bulk composition is same as Fig. 9 of White et al. (2014b). The thermodynamic dataset used was Holland and Powell (2011), ds6.2. The a-x models are those used in White et al.. (2014). The version of Perple_X is v6.9.0, the initial_resolution = [1/6, 1/16], all other option values are default. The dotted lines are from Fig. 9 of White et al. (2014) which are calculated by THERMOCALC.

Figure S6. A *P–T* phase diagram for a metapelitic rock using Theriak-Domino. The bulk composition is same as Fig. 9 of White et al. (2014b). The thermodynamic dataset used was Holland and Powell (2011), ds6.2. The a-x models are those used in Green et al. (2016). The executables of Theriak-Domino are from http://dtinkham.net/peq.html. The dotted lines are from Fig. 9 of White et al. (2014) which are calculated by THERMOCALC.

Figure S7. A *P*–*T* phase diagram for KLB-1 calculated using GeoPS. The bulk composition is same as Fig. 1 of Jennings et al. (2015). The thermodynamic dataset used was Holland and Powell (2011), ds6.22. The a-x models are those used in Jennings et al. (2015).

Figure S8. A *P*–*T* phase diagram for KLB-1 calculated using Perple_X. The bulk composition is same as Fig. 1 of Jennings et al. (2015). The thermodynamic dataset used was Holland and Powell (2011), ds6.2. The a-x models are those used in Jennings et al. (2015). The version of Perple_X is v6.9.0, the initial_resolution = [1/6, 1/16], all other option values are default.

How to cite this article: Xiang, H., & Connolly, J. A. D. (2021). GeoPS: An interactive visual computing tool for thermodynamic modelling of phase equilibria. *Journal of Metamorphic Geology*, 1–13. https://doi.org/10.1111/jmg.12626